Available online at www.sciencedirect.com
SCIENCE DIRECT®
Communications in Nonlinear Science and Numerical Simulation 10 (2005) 907–920
Communications in Nonlinear Science and Numerical Simulation
www.elsevier.com/locate/cnsns

Applying proper orthogonal decomposition to the computation of particle dispersion in a two-dimensional ventilated cavity

C. Allery *, C. Béghein, A. Hamdouni

LEPTAB, Université de La Rochelle, Avenue Michel Crépeau, 17042 La Rochelle Cédex 1, France

Received 12 March 2004; accepted 24 May 2004
Available online 23 July 2004

Abstract

The Lagrangian technique is used to compute particle dispersion in a two-dimensional ventilated cavity. The instantaneous air velocity field at the particle's location is obtained by proper orthogonal decomposition (POD). The low-dimensional dynamic model is obtained by performing a Galerkin projection of the Navier–Stokes equations onto each POD eigenfunction and it is coupled with the particle's equation of motion. A substantial decrease in computing time (when comparing with LES computations) is noted. Two different cases of particles' injection are modelled: the particle source is located in the inlet in the first simulation, and close to the floor in the second simulation.

PACS: 47.27.i; 47.55.Kf; 05.45.a
Keywords: Lagragian technique; Low-order dynamical system; POD; Particle dispersion

1. Introduction

Nowadays people spend a great amount of time in an indoor environment and it is thus important to predict indoor air quality in order to assess health risks. Indoor air quality may be related

* Corresponding author. Tel.: +33 5 46 45 86 22; fax: +33 5 46 45 82 41.
E-mail address: callery@univ-lr.fr (C. Allery).

1007-5704/$ - see front matter
doi:10.1016/j.cnsns.2004.05.005

to gaseous pollutants (volatile organic compounds, formaldehyde for instance) and also to particles (tobacco smoke, black carbon soot emitted by motor vehicles...). Our work is more particularly focused on the numerical modelling of particle dispersion in a ventilated cavity. The long term objective is to control particle dispersion in an active way, for realistic configurations encountered in buildings. In the present paper, a Lagrangian particle tracking method is used in conjunction with a low-order dynamical system obtained by proper orthogonal decomposition (POD) that provides the fluid flow dynamics.

Using the Lagrangian technique to compute particle dispersion in a turbulent flow requires the knowledge of the instantaneous fluid velocity at the particle's location. The instantaneous velocity can be obtained in three different ways. The first one is direct numerical simulation [1–3]. In this approach, Navier–Stokes equations are solved numerically without using a turbulence model. The mesh should be fine enough to solve the smallest scales of motion, this approach is therefore very time consuming and cannot be applied to building simulation. Another approach is to use Reynolds averaged Navier–Stokes models to compute the time averaged turbulent flow, and to introduce a stochastic model that provides the fluctuating velocity field [4–6]. These models are generally formulated for homogeneous turbulence and their extension to more complex flows is a hard task. The last approach consists in using large eddy simulation (LES) to generate the instantaneous flow information [7–9]. With LES, a filter is applied to Navier–Stokes equations. The instantaneous velocity of the eddies larger than the filter length scale is computed, and the effect of the subgrid scales is modelled. Applying LES to compute particle dispersion in a room is nevertheless a computationally intensive technique. To compute particle dispersion in a turbulent flow with LES it is necessary to couple at the same time step the computation of the instantaneous velocity field and the particle dispersion. Small time steps are required to integrate the particles' equations of motion, and a large amount of time step must be used when dealing with indoor air quality.

In the 1980s, researchers have developed low-dimensional dynamic models to compute turbulent flows at a reduced cost. One of the most widely used techniques is proper orthogonal decomposition that is based on the construction of an optimal basis function (in an energetic norm sense). In the present study, the instantaneous velocity of the turbulent flow is computed by the means of POD in a first step, and a coupled system of differential equations (composed of the particles' equation of motion and the equation of the instantaneous fluid velocity at the particles' location by POD) is solved in order to get the particles' velocity and position. This principle was already applied to investigate the motion of bubbles and particles in a turbulent boundary layer [10]. Experimental results were used to construct the POD basis. Only one POD mode was used in the wall-normal direction, and Fourier modes were used in the spanwise and streamwise directions.

This contribution considers the investigation of particle dispersion in a ventilated cavity. Since this work is in its early stages, the flow is assumed isothermal and two-dimensional. Moreover, it is heterogeneous according to the two space directions. The POD basis is derived by first computing the turbulent flow with two-dimensional large eddy simulation. It should be pointed out here that although the use of two-dimensional LES may be somewhat questionable, it has been applied successfully to other types of flows [11,12]. The ability of the POD basis to reproduce the turbulent flow is tested. The low-dimensional dynamic model is obtained by performing a Galerkin projection of Navier–Stokes equations onto each eigenfunction and it is coupled with the particles' equation of motion. A substantial decrease in computing time (when comparing with LES computations) is noted. The influence of the number of particles injected in the flow on particles' sta-

tistical results is analyzed. Two different cases of particles' injection are modelled: the particle source is located in the inlet in the first simulation, and close to the floor in the second simulation. In the last part of this paper, the implementation of this code on an IBM SP supercomputer is explained, and the low cost computations of the simulations are highlighted.

2. POD method

The proper orthogonal decomposition (POD) is inspired by the principal component analysis (PCA) in data processing. The main idea of PCA is to reduce the dimensionality of data set which consists of a large number of interrelated variables, while retaining as much as possible the variation present in the data set. This is achieved by transforming the original variables into a new set of variables, the principal components, which are uncorrelated and are ordered so that the first few ones retain most of the variation present in all of the original variables. POD is thus a powerful technique for extracting basis functions that represent ensemble averaged structures. This technique, which was introduced in fluid mechanics by Lumley [13] in 1967, has been found to be useful and efficient in approximating the dynamics of flows characterized by large-scale spatially coherent structures. As a very small number of POD modes capture most of the energy, this technique is also used to construct low-dimensional dynamic models. A Galerkin projection of the Navier–Stokes equations onto the most energetic POD modes gives a low finite-dimensional system of non-linear ordinary differential equations (ODE) for which solution can be found with a very limited computational effort when compared to DNS or LES of a turbulent flow. Since 1988 and the pioneering paper of Aubry et al. [14] in which the motion of structures in the wall region of a flat plate turbulent boundary layer was represented by a realistic dynamical system, the construction of low-dimensional models has been considered for numerous configurations such as flows in driven cavities [15,16], in boundary layers [17], in plane mixing layers [18], across sudden expansions [11,19].

2.1. Proper orthogonal decomposition

The basic idea of POD consists in finding a "physical" basis which is optimal in an energetic sense. Thus, we search a deterministic function ϕ which gives the "best" representation of the set of flow fields $\mathbf{u}$ (assumed random and at real values) in the following sense:

$$\begin{cases} \overline{(\mathbf{u},\phi^2)} = \max_{\psi\in L^2(\Omega)} \overline{(\mathbf{u},\psi^2)} \\ (\phi,\phi) = 1 \end{cases} \tag{1}$$

where $(\bullet,\bullet)$ denotes the inner product of $L^2(\Omega)$ and $\bar{\bullet}$ denotes a statistic average operator. L^2 is the space of functions of finite energy in the flow volume Ω.

From variational calculus it follows that the above expression is equivalent to the Fredholm integral

$$\text{Find } \lambda\in\mathbb{R} \quad \text{and} \quad \phi\in L^2(\Omega) \quad \text{with} \quad \int_\Omega R(\boldsymbol{x},\boldsymbol{x}')\phi(\boldsymbol{x}')\,\mathrm{d}\boldsymbol{x}' = \lambda\phi(\boldsymbol{x}) \tag{2}$$

representing an eigenvalue problem for ϕ. R is the spatial correlation tensor defined, with ergodicity hypothesis, by:

$$R(\boldsymbol{x},\boldsymbol{x}') = \overline{\mathbf{u}(\boldsymbol{x},t)\otimes\mathbf{u}(\boldsymbol{x}',t)} \tag{3}$$

The eigenfunctions ϕ_n are orthogonal and all realizations of the flow $\mathbf{u}$ are written as:

$$\mathbf{u}(\boldsymbol{x},t) = \sum_{n=1}^{+\infty} a_n(t)\phi_n(\boldsymbol{x}) \text{ in } L^2(\Omega) \text{ sense, with } a_n(t) = (\mathbf{u}(\boldsymbol{x},t),\phi_n) \tag{4}$$

In practice, if the sampling of the flow field is obtained by numerical simulation, the evaluation of the tensor R is a very large computational task. In order to reduce the calculation, we used the Snapshots method proposed in 1987 by Sirovich [20]. In this technique, based on the fact that the eigenfunctions can be expressed in terms of the original set of data,

$$\phi_n(\boldsymbol{x}) = \sum_{k=1}^{M} \mathbf{u}(\boldsymbol{x},t_k)A_{nk} \tag{5}$$

we must solve the matrix eigenvalue problem:

$$\sum_{k=1}^{M} C_{kj}A_{nk} = \lambda A_{nj} \quad \text{for } j = 1,\ldots,M \tag{6}$$

where A_{nk} denotes the constants associated to the nth mode, M is the number of snapshots, and C is the temporal correlation tensor defined by:

$$C_{kj} = \frac{1}{M}\int_{\Omega} u_i(\boldsymbol{x},t_k)u_i(\boldsymbol{x},t_j)\,\mathrm{d}x \tag{7}$$

As C is symmetric and positive semi-definite, all eigenvalues are real and non-negative and can be ordered as $\lambda_1 \geqslant \lambda_2 \cdots \geqslant \lambda_M$. Each eigenvalue λ_n, taken individually, represents the energy contribution of the corresponding eigenfunction. The eigenvectors ϕ_n are by construction incompressible (e.g. their divergence is null), satisfy the boundary conditions and can be normalized to form an orthonormal set. The main property of the POD is its ability to give the best approximation of the flow in an energetic sense [21]. The energy contained in the first N POD modes is indeed always greater than the energy contained in any other basis such as the Fourier basis.

2.2. Low-order dynamical system

Usually, the first N (N small) POD modes contain most of the energy. So we can expect that a low-order dynamical system, obtained by Galerkin projection of the Navier–Stokes equations onto the most energetic eigenmodes ϕ_n, gives the flow dynamics accurately. The first step consists in approximating the flow field $\mathbf{u}$ by keeping the first N modes and ignoring the remaining modes. This approximation is written as:

$$\mathbf{u}(\boldsymbol{x},t) \simeq \sum_{n=1}^{N} a_n(t)\phi_n(\boldsymbol{x}) \tag{8}$$

The second step consists in performing a Galerkin projection. As the continuity equation for incompressible flow is satisfied by each eigenfunction, we only consider the dimensionless momentum equation of the flow:

$$\frac{\partial u}{\partial t} + \mathbf{u}\cdot\nabla\mathbf{u} = -\nabla P + \frac{1}{Re}\Delta\mathbf{u} \tag{9}$$

where Re and P are respectively the Reynolds number and the pressure. Introducing (8) into Eq. (9), projected onto the spatial structures ϕ_n, and taking ϕ orthonormal:

$$\frac{\mathrm{d}a_n}{\mathrm{d}t} = \sum_{m=1}^{N}\sum_{k=1}^{N} C_{nmk} a_m a_k + \sum_{m=1}^{N} B_{nm} a_m + D_n \quad \text{with } n = 1,\ldots,N \tag{10}$$

and $C_{nmk} = -(\phi_n, \nabla\phi_m \cdot \phi_k)$, $B_{nm} = \dfrac{1}{Re}(\phi_n, \Delta\phi_m)$, $D_n = -\int_\Gamma P\phi_n \mathbf{n}\,\mathrm{d}S$ where $\mathbf{n}$ is the outward normal on the domain Ω considered of boundary Γ.

The previous system of equations includes a term D_n that is linked to the pressure P. But there is no simple expressions of this term according to the expansion coefficients ϕ_n. This term should be known for each time step when integrating (10). This is quite difficult to achieve, but for a few configurations, D_n is strictly equal to 0 (in a driven cavity for instance, because the ϕ_n functions are null on the boundaries) or is assumed to be 0. To overcome this difficulty, if this term cannot be neglected, various approaches have been considered. This term was modelled by Aubry et al. [14] for the study of the viscous sublayer in a channel flow. This modelling technique cannot be extended to other flow configurations. On another hand, Rempfer [17] proposed to use a vorticity formulation of the problem. Since this formulation induces a higher order derivative, it generates a numerical noise which disturbs the prediction of the dynamical system. To avoid this term, Allery [22] uses a stress formulation in conjunction with a penalization of the non-homogeneous Dirichlet boundary conditions, for studying the flow through a long diffuser.

The POD method can be applied to the instantaneous field ($\mathbf{u}$ and P) or to the fluctuating field. In this section, in order to simplify the notations, the technique has been presented for the instantaneous field. If the fluctuating field is considered, the dynamical system is slightly modified. It is obtained by decomposing the instantaneous velocity and pressure fields into a mean component $\bar{\bullet}$, with the fluctuating part of the velocity $\bullet'$ expressed according to the POD basis. This yields:

$$\begin{cases} \mathbf{u}(\boldsymbol{x},t) = \overline{\mathbf{u}}(\boldsymbol{x}) + \mathbf{u}'(\boldsymbol{x},t) \simeq \overline{\mathbf{u}}(\boldsymbol{x}) + \sum_{n=1}^{N} a_n(t)\phi_n(\boldsymbol{x}) \\ P(\boldsymbol{x},t) = \overline{P}(\boldsymbol{x}) + P'(\boldsymbol{x},t) \end{cases} \tag{11}$$

These expressions are then introduced into the Navier–Stokes equations. The coefficients' expression is detailed in [15,22].

3. Particle model

A monodisperse aerosol in an isothermal flow is considered here. The particles are solid and spherical. Aerosols in buildings are dilute. The particles do not modify the flow and do not coagulate, a one-way coupling approach is thus used. The Lagrangian approach is employed in order to compute the particles' trajectories. A large amount of particles should be released in the flow in order to obtain statistically independent results. Since the density ratio (particle density versus gas density) is rather high (about 2000), the particles are mainly submitted to the gravity and drag forces. Other forces such as the buoyancy force, the added mass effect and the Basset force are negligible. As in a previous study performed by Ahmadi and Li [23], the Saffman lift force is not considered because the particle studied here are rather small (5 μm diameter). In addition, the particles do not exhibit a random motion due to Brownian effects, because the particle diameters in this study are greater than 1 μm. The particle equation of motion is therefore:

$$\rho_p \frac{\pi d_p^3}{6} \frac{d\mathbf{u}_p}{dt} = \frac{\pi d_p^3}{6} \rho_p \mathbf{g} + \frac{\pi d_p^2}{8} \rho C_d \|\mathbf{u} - \mathbf{u}_p\| (\mathbf{u} - \mathbf{u}_p) \tag{12}$$

where ρ_p, d_p, $\mathbf{u}_p$ are the density, diameter and velocity of the particle, g is the gravitational acceleration, ρ is the fluid density and $\mathbf{u}$ is the instantaneous fluid velocity at the particle's location. According to Hinds [24], the drag coefficient can be calculated as a function of the particle Reynolds number Re_p in the following manner:

$$\begin{cases} C_d = \dfrac{24}{Re_p} & \text{if } Re_p < 1 \\ C_d = 0.44 & \text{if } Re_p > 1000 \\ C_d = \dfrac{24}{Re_p}\left(1 + \dfrac{Re_p^{2/3}}{6}\right) & \text{if } 1 < Re_p < 1000 \end{cases} \tag{13}$$

with $Re_p = \dfrac{\|\mathbf{u} - \mathbf{u}_p\| d_p}{v}$ and v is the kinematic fluid viscosity.

Eq. (12) is solved at each time step for each particle. Integrating this equation according to time yields the particle velocity. The particle position at each time step is obtained by integrating:

$$\mathbf{u}_p = \frac{d\boldsymbol{x}_p}{dt} \tag{14}$$

In a previous study, the instantaneous fluid velocity at the particle's location was obtained by performing large eddy simulation at each time step [25], and this three-dimensional model was successfully validated by comparison of the numerical results with the experimental results of Snyder and Lumley [26]. This approach requires a large amount of computing time, because the time step should be very small (it is imposed by the explicit integration of the particle's equation of motion). In this work, the instantaneous fluid velocity at the particle's location is provided by the proper orthogonal decomposition method, so combining Eqs. (10), (12) and (14) yields the following coupled problem

$$\begin{cases} \dfrac{d\mathbf{a}}{dt} = F(\mathbf{a}, t) \\ \dfrac{d\mathbf{u}_p}{dt} = G(\mathbf{a}, \mathbf{u}_p, t) \\ \dfrac{d\boldsymbol{x}_p}{dt} = \mathbf{u}_p \end{cases} \tag{15}$$

where $\mathbf{a} = (a_1, \ldots, a_n)$. This set of differential equations is solved by the Runge–Kutta method.

4. Results

4.1. Description of the case study

The application case considered here is particle dispersion in an isothermal two-dimensional ventilated cavity (see Fig. 1). The inlet is located in the upper part of the left wall (0.31 m beneath

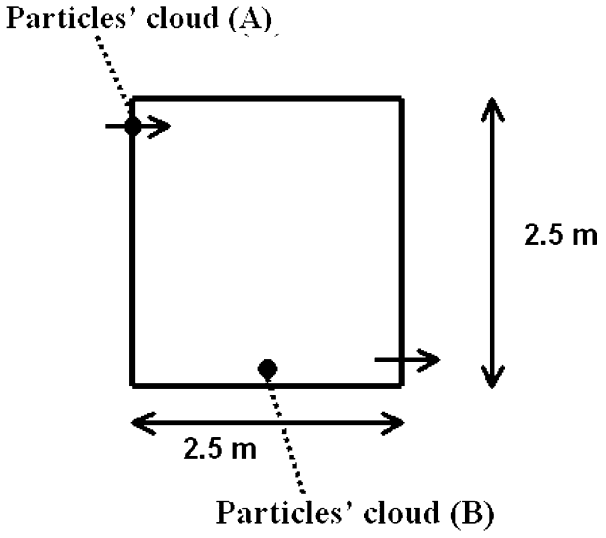

Fig. 1. Geometry of the ventilated cavity.

the ceiling) and the outlet is in the lower part of the right wall (0.31 m above the floor). The room dimensions are 2.5 m long and 2.5 m high. The inlet height is 0.07 m and the outlet height 0.07 m, the mean velocity and turbulent intensity at inlet are respectively 0.443 m/s and 10%. The turbulent flow has been computed by using the STAR-CD code. The LES model selected is the one-equation subgrid k model that comprises a balance equation for the subgrid kinetic energy [27] (written in tensorial notation).

$$\begin{cases} \dfrac{\partial k}{\partial t} + \dfrac{\partial}{\partial x_j}(\tilde{u}_j k) = v_t P_k + \dfrac{\partial}{\partial x_j}\left(v_t \dfrac{\partial k}{\partial x_j}\right) - C_\varepsilon \dfrac{k^{3/2}}{\Delta} \\ P_k = \left(\dfrac{\partial \tilde{u}_j}{\partial x_i} + \dfrac{\partial \tilde{u}_j}{\partial x_i}\right)\dfrac{\partial \tilde{u}_i}{\partial x_j} \end{cases} \tag{16}$$

where $\tilde{u}_j$ is the resolved large-scale velocity component, v_t is the subgrid scale viscosity

$$v_t = C_k \Delta \sqrt{k} \tag{17}$$

Δ is the filter width which separates the resolved scales from subgrid scales, and the dimensionless model coefficients are given the values

$$C_k = 0.05, \qquad C_\varepsilon = 1.00 \tag{18}$$

The flow domain was discretized into a non-uniform mesh of 18 477 cells. A time step equal to 0.005 s ensured a CFL (Courant–Friedrichs–Lewy condition) less than 0.5.

Since POD enables a high reduction in computing time, many cases of particle dispersion can be considered with a minimum of effort unlike with LES or DNS. As this paper is devoted to highlight the ability of POD to compute particles' dispersion, we focused on two cases of particles' injection. In the first simulation, denoted (A) in Fig. 1, a cloud of 10 000 particles (diameter $d_p = 5$ μm, density $\rho_p = 2000$ kg/m^3) was released in the middle of the inlet at the same time. In

the second simulation, denoted (B) in Fig. 1, the same cloud of particles was injected 10 cm above the floor. For these two cases the initial particles' velocity was set equal to the instantaneous fluid velocity. The time step chosen for particle computation was 0.0002 s. 150 000 time steps were performed for simulations (A) and (B). For the cases studied in this paper, the particles were supposed to be attached to the wall when they contacted the surfaces.

4.2. POD application

Once the LES computation of the turbulent flow has converged, POD was applied to the fluctuating fields and 99 snapshots of velocity ($M=99$) fields were recorded every 0.01 s. In Table 1 the percentage of fluctuating energy E_n contained in the mode n, and the cumulative energy E_c contained in the n first POD modes are presented. They are defined according to:

$$E_n = \lambda_n \Big/ \sum_{i=1}^{M} \lambda_i \qquad \text{and} \quad E_c = \sum_{i=1}^{n} \lambda_i \Big/ \sum_{i=1}^{M} \lambda_i \tag{19}$$

Table 1 shows that only one mode contains 78% of energy and with four modes the fluctuating energy of the signal is almost captured.

The ability of the first POD modes to reproduce the flow velocity, was then tested. The following normalized residual was considered:

$$\mathrm{res}(n) = \frac{\|\beta\|_\infty}{\|\eta\|_\infty} \tag{20}$$

with $\beta^2 = \int_\Omega \left[\mathbf{u}(x,t) - \sum_{k=1}^{n} a_k(t)\phi_k(x)\right]^2 \mathrm{d}x$ and $\eta^2 = \int_\Omega [\mathbf{u}(x,t)]^2 \mathrm{d}x$. Here $\|\bullet\|_\infty$ is the infinite norm, $\|f(t)\|_\infty = \sup f(t)$.

Fig. 2 indicates that only four modes are necessary to obtain a residual less than 1.8×10^{-2} (which corresponds to a relative error of 3.2×10^{-4}). With four modes the fluctuating velocities are hence well reconstructed. Therefore, the low-order system, used to compute the flow dynamics and the particle dispersion, is obtained with four modes.

4.3. Reduced model

Fig. 3 shows the temporal evolution of the modes $a_n(t)$ during the sampling time used for the snapshot method. In this figure, POD corresponds to the reference solution obtained by projecting the LES velocity field onto the spatial structure ϕ_n, *pressure* and *without pressure* are the coef-

Table 1
Energy contained in the first eigenvalues λ_n of the POD

Mode n	λ_n	$100E_c$	$100E_n$
1	0.53399E−02	78.62948	78.62948
2	0.98829E−03	93.18179	14.55231
3	0.29199E−03	97.48127	4.29948
4	0.96186E−04	98.89760	1.41632
5	0.33250E−04	99.38720	0.48960

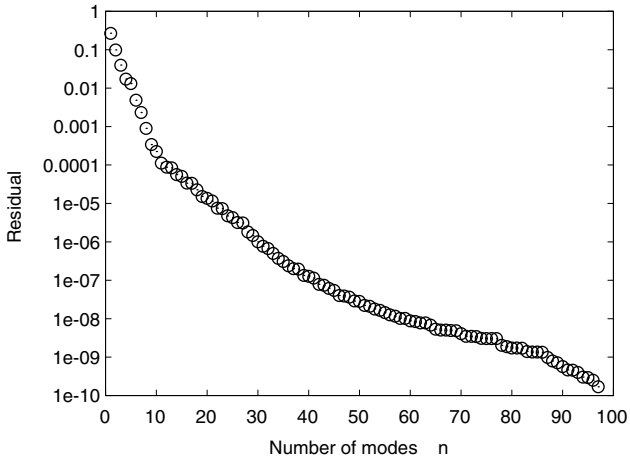

Fig. 2. Evolution of the POD residual according to the number of mode n kept in the reconstruction.

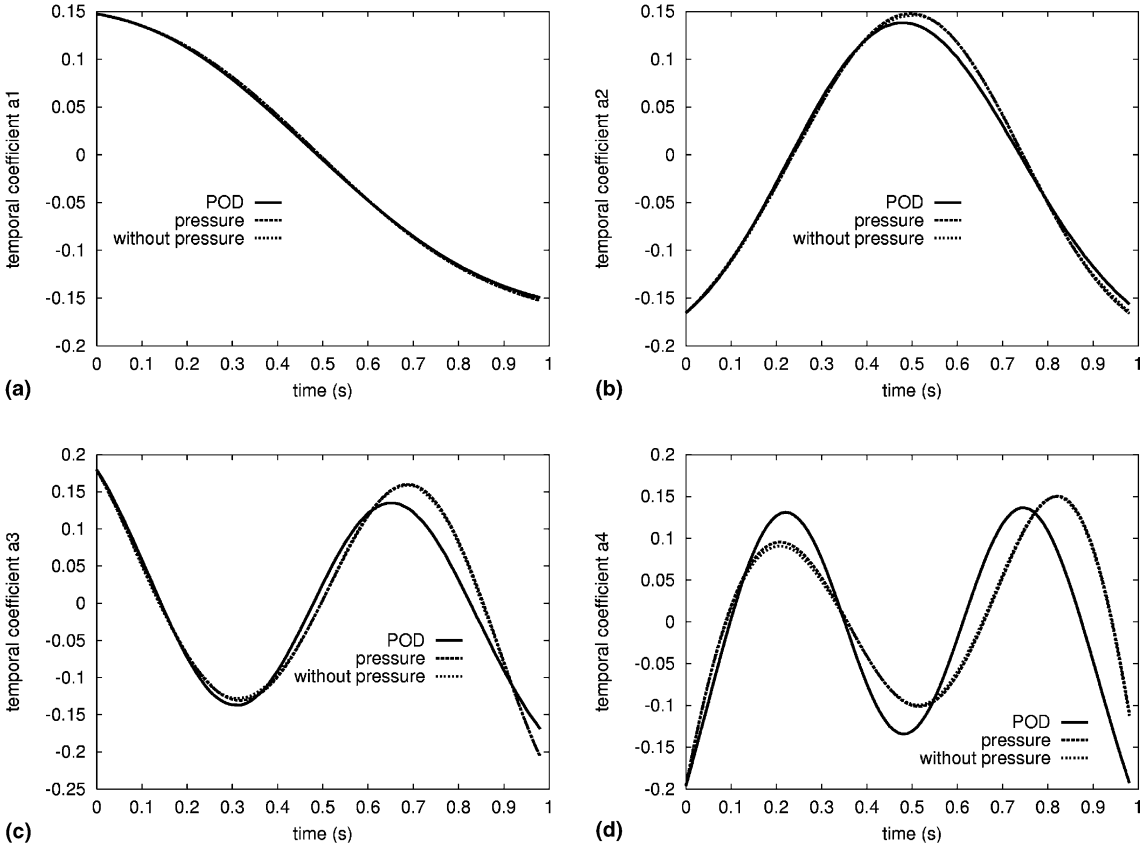

Fig. 3. Temporal evolution of the four modes obtained by integration of the dynamical system: (a) mode 1, (b) mode 2, (c) mode 3 and (d) mode 4.

ficient obtained by solving the dynamical system (10) respectively with the pressure term included, and without the pressure term. It can be noticed that the temporal evolution of the reference functions POD are properly recovered from the dynamical system. These figures also highlight that not considering the pressure term in the dynamical system does not affect the prediction of the mode $a_n(t)$. This term will thus be neglected in the next paragraphs.

While the POD basis was built with 1 s of the fluctuating flow computed with LES, particle dispersion was calculated for a duration of 30 s, with the low-order dynamical system.

4.4. Particle dispersion in the ventilated room

Fig. 4 gives instantaneous streamlines of the flow. The main features of the cavity flow are as the usual ones encountered in a ventilated cavity. The cavity flow consists of small recirculation regions in the corners of the cavity and a big one in the room core.

Fig. 5 presents the temporal evolution of the particles' cloud for the configuration (A). The particles followed the jet path. About 2 s since the particles' injection, the particles were lifted in the small recirculation region located in the upper left part of the room (Fig. 5(a)). The same phenomenon was observed in a previous study of particles' dispersion computed with 3D LES [25]. Fig. 5(b) shows the particles going down along the right wall. In Fig. 5(c) and (d), it can be noticed that some particles were exhausted. Fig. 6(a) confirms this assertion. Fig. 6(b) also highlights that a few particles were eliminated because they were attached to the walls (and more particularly on the right and left vertical walls). In Fig. 5(d), it can be seen that 30 s since the particles' injection, the indoor air quality was rather bad, many particles diffused to the core region.

An advantage of using POD to compute the instantaneous air velocity field is that many cases of particles' injection can be investigated without re-computing the turbulent flow. Starting from

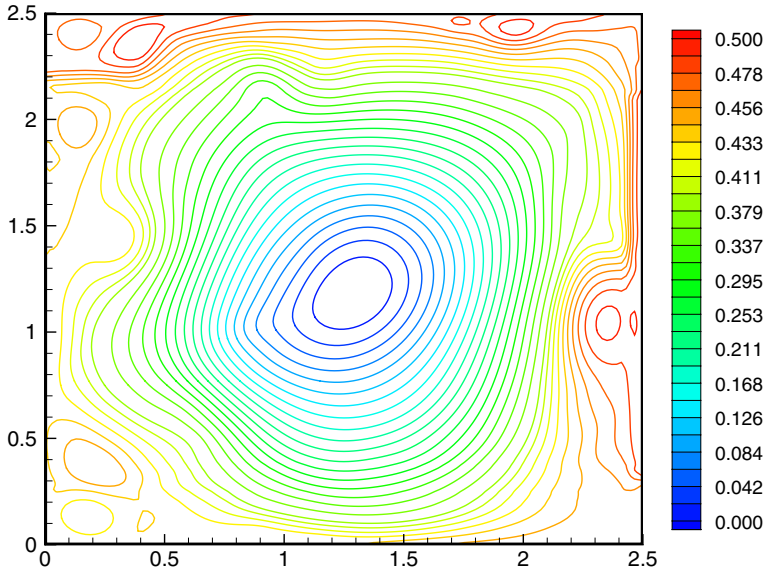

Fig. 4. Instantaneous streamlines at the beginning of the particles' release.

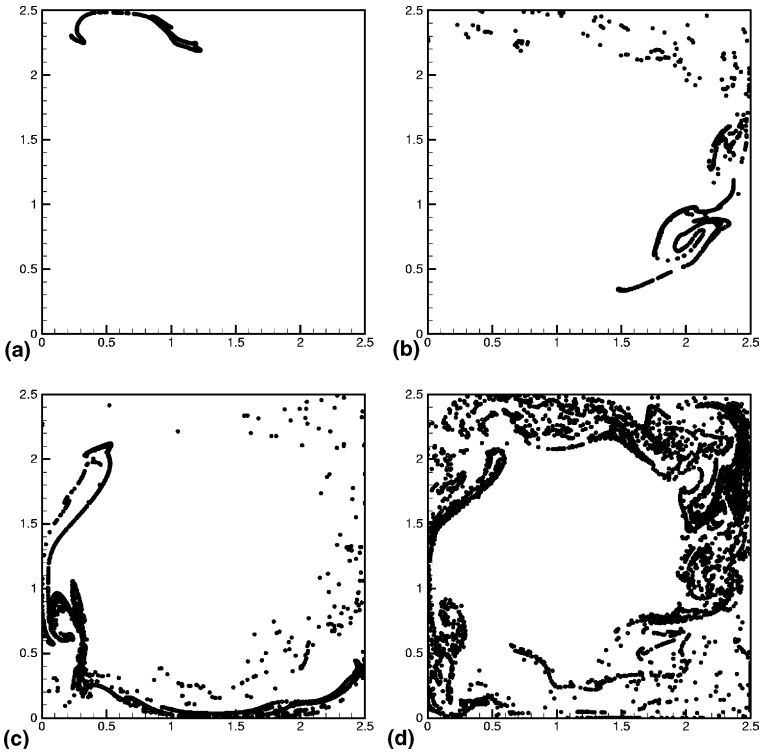

Fig. 5. Temporal evolution of the particles' cloud (A) in the room: (a) 4 s, (b) 12 s, (c) 20 s and (d) 30 s.

the same instantaneous velocity field as in the previous case, we studied the influence of the location of the particles' attack. In this case, the particles' source was located very close to the floor. Fig. 7 shows the same features as in Fig. 5. The particles were lifted by the airflow. They followed the main circular air path, some of which moved in the small recirculation regions (see Fig. 7(b)). Since the particles were released very close to the floor, the greatest part of the attached particles were located on the left wall (see Fig. 7(b) and (c)). For this configuration, 30 s since the particles' injection, the indoor air quality is also rather bad.

4.5. Implementation on a parallel computer

At each time step, only four differential equations were solved to compute the turbulent flow, but a large number of differential equations were used to get the particles' trajectories (four equations for one particle, which implies for instance 40 000 equations if 10 000 particles are injected in the turbulent flow). Moreover the particles do not interact with each other. It was thus interesting to parallelize the particles' loop. The code was implemented on an IBM SP supercomputer and parallelized with MPI (Message Passing Interface). A SPMD (Single Program Multiple Data) approach is employed (the same program is at once master and slave). Each processor computes the turbulent flow and executes the same particles' loop for $N_{\text{part}}/N_{\text{proc}}$ particles where N_{part} is the number of particles and N_{proc} is the number of processors. At the end the host processor collects

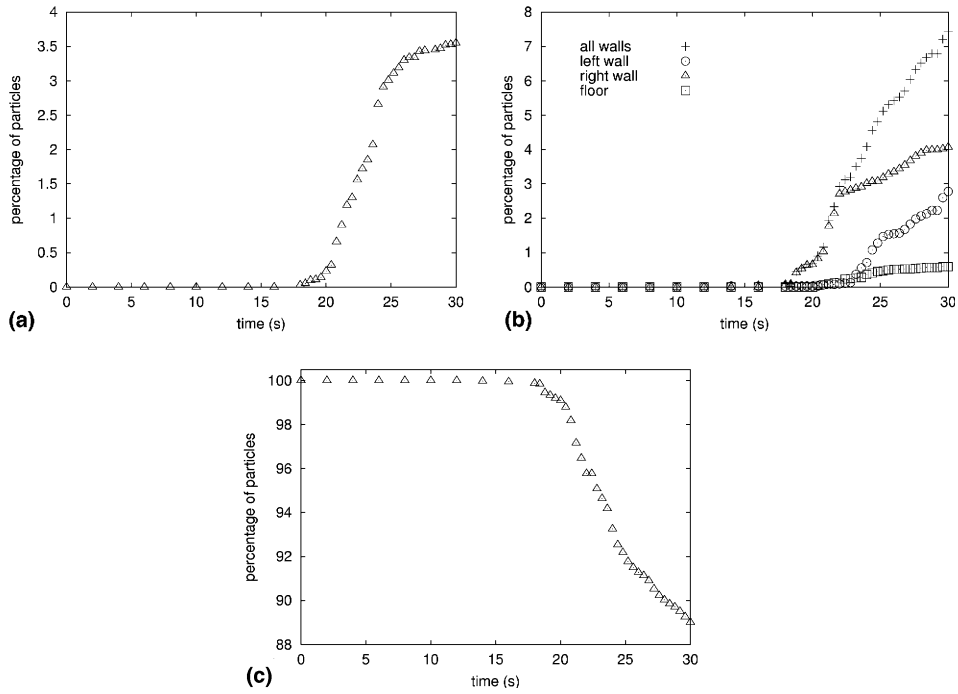

Fig. 6. Percentage of particles in the room over time (configuration (A)): (a) percentage of particles exhausted, (b) percentage of attached particles and (c) percentage of particles in the air flow.

the results of all N_{part} independent trajectories and calculates the statistical results (percentage of particles in the room, attached to each wall, ...).

We noticed that POD is a technique which considerably decreases the computing time. While 19 days were necessary to compute the dispersion of 1000 particles with 3D large eddy simulation, only 3 days and 10 h were needed to deal with the dispersion of 10000 particles obtained by 2D proper orthogonal decomposition. In addition, the particles' loop in the 3D LES program was parallelized, but since the program spends most of the time computing the turbulent flow with LES, the parallelization is not efficient. This is not the case with POD. The computation of particles' dispersion with POD required only 12 h with 10 processors.

5. Conclusion

In this paper, we presented a numerical study of particle dispersion in a ventilated room computed by means of proper orthogonal decomposition. A two-dimensional configuration was considered here as a first step. Similar features as ones noticed when computing particle dispersion in a three-dimensional ventilated room with large eddy simulation, were highlighted. The behavior of our model is therefore qualitatively satisfactory. We are now extending this model in order to treat three-dimensional configurations. This will enable us to validate this model in a quantitative way, by comparing our results with ones obtained with our model based on the computation of

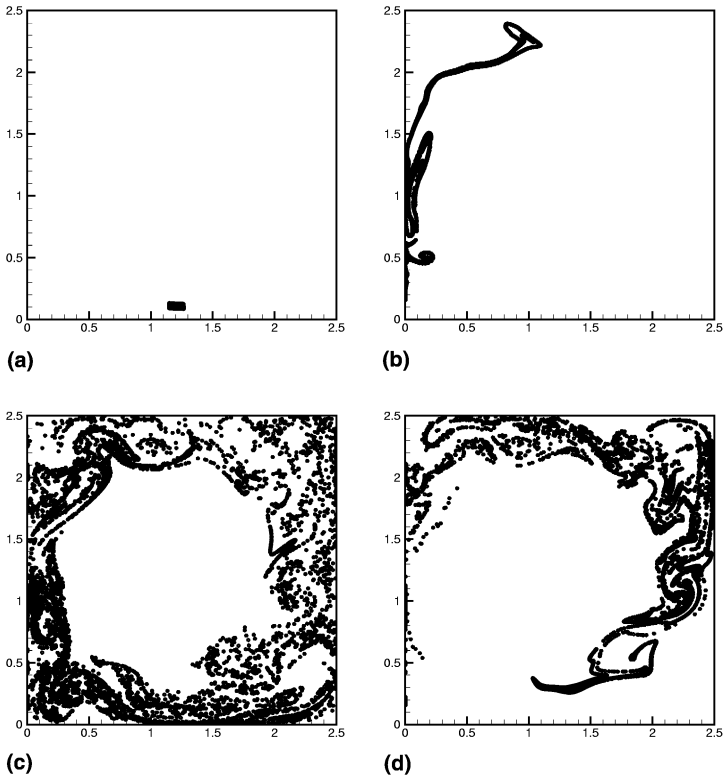

Fig. 7. Temporal evolution of the particles' cloud (B) in the room: (a) 0 s, (b) 12 s, (c) 20 s and (d) 30 s.

particle dispersion with large eddy simulation. A particular attention will be paid to the behavior of particles in the vicinity of walls. Moreover, proper orthogonal decomposition has been shown here to be a powerful tool to save a very large amount of computing time as well as computer memory. A substantial decrease in computing time may be also obtained by solving the coupled dynamical system (POD and particles) by using the asymptotic numerical method (ANM), which consists in finding the solution as a formal series according to time.

Acknowledgement

The authors wish to express their thanks to the CINES (Centre Informatique National de l'Enseignement Supérieur). The computations were performed with the IBM SP of the CINES.

References

[1] Armenio V, Fiorotto V. The importance of the forces acting on particles in turbulent flows. Phys Fluids 2001;13(8):2437–40.
[2] Chen M, McLaughlin JB. A new correlation for the aerosol deposition rate in vertical ducts. J Colloid Interface Sci 1995;169:437–55.

[3] Thakurta DG, Chen M, McLaughlin JB, Kontomaris K. Thermophoretic deposition of small particles in a direct numerical simmulation of turbulent channel flow. Int J Heat Mass Transfer 1998;41:4167–82.
[4] Desjonquères P, Berlemont A, Gouesbet G. A Lagrangian approach for the prediction of particle dispersion in turbulent flows. J Aerosol Sci 1988;19(1):99–103.
[5] Gosman AD, Ioannides E. Aspects of computer simulation of liquid-fuelled combustors. Paper presented at the AIAA 19th Aerospace Science Mtg, St Louis, MO, paper 81-0323.
[6] Sommerfeld M, Kohnen G, Rüger M. Some open questions and inconsistencies of Lagrangian particle dispersion models. Paper presented at the Ninth Symposium on Turbulent Shear Flows, Kyoto, August 1993, paper 15.1.
[7] Armenio V, Piomelli U, Fiorotto V. Effect of the subgrid scales on particle motion. Phys Fluids 1999;11(10):3030–42.
[8] Pandya RVR, Mashayek F. Two-fluid large eddy simulation approach for particle-laden turbulent flows. Int J Heat Mass Transfer 2002;45(24):4753–9.
[9] Yeh F, Lei U. On the motion of small particles in a homogeneous isotropic turbulent flow. Phys Fluids 1991;3(11):2571–86.
[10] Joia IA, Ushijima T, Perkins RJ. Numerical study bubble and particle motion in a turbulent boundary layer using proper orthogonal decomposition. Appl Sci Res 1997;57:263–77.
[11] Allery C, Guérin S, Hamdouni A, Sakout A. Experimental and numerical POD study of the Coanda effect used to reduce self-sustained tones. Mech Res Commun 2004;31(1):105–20.
[12] Yu KF, Lau KS, Chan CK. Large eddy simulation of particle-laden turbulent flow over a backward-facing step. Commun Nonlin Sci Numer Simul 2004;9:251–62.
[13] Lumley JL. The structure of inhomegeneous turbulent flows. In: Monin AM, Tararsky VI, editors. Atmospheric Turbulence and Wave Propagation. Moscow: Nauka; 1967. p. 166–78 [in Russian].
[14] Aubry N, Holmes P, Lumley JL, Stone E. The dynamics of coherent structures in the wall region of a turbulent boundary layer. J Fluid Mech 1988;192:115–73.
[15] Cazemier W, Verstappen RW, Veldman AEP. Proper orthogonal decomposition and low dimensional models for driven cavity flows. Phys Fluids 1998;10(7):1685–99.
[16] Jorgensen BH, Sorensen JS. Proper orthogonal decomposition and low-dimensional modeling. Ercoftac 2000;46:44–51.
[17] Rempfer D. Investigations of boundary layer transition via Galerkin projections on empirical eigenfunctions. Phys Fluids 1996;8(1):175–88.
[18] Ukeiley L, Cordier L, Manceau R, Delville J, Glauser M, Bonnet JP. Examination of large-scale structures in a turbulent plane mixing layer. Part 2. Dynamical systems model. J Fluid Mech 2001;441:67–108.
[19] Gunes H. Low dimensional modeling of non-isothermal twin-jet flow. Int Commun Heat Mass Transfer 2002;29(1):77–86.
[20] Sirovich L. Turbulence and the dynamics of coherent structures. Part 1: Coherent structures. Part 2: Symmetries and transformations. Part 3: Dynamics and scaling. Quart Appl Math 1987;45:561–90.
[21] Berkooz G, Holmes P, Lumley JL. The proper orthogonal decomposition in the analysis of turbulent flows. Ann Rev Fluid Mech 1993;25:539–75.
[22] Allery C. Contribution à l'identification des bifurcations et à l'étude des écoulements fluides par des systèmes dynamiques d'ordre faible (P.O.D.). Phd thesis, University of Poitiers, France, 2002 [in French].
[23] Ahmadi G, Li A. Computer simulation of particle transport and deposition near a small isolated building. J Wind Eng Ind Aerodyn 2000;84:23–46.
[24] Hinds WC. Aerosol technology: properties, behaviour, and measurement of airborne particles. New York: John Wiley; 1982.
[25] Jiang Y, Béghein C, Chen Q. Study of particle dispersion in buldings with large-eddy simulation. Paper presented at the Ninth International Conference on Indoor Air Quality and Climate (Indoor Air 2002) Monterey, CA, June 30–July 5, 2002, paper 4C405.
[26] Snyder WH, Lumley JL. Some measurements of particle velocity autocorrelation functions in a turbulent flow. J Fluid Mech 1971;48(1):41–71.
[27] Fureby C, Tabor G, Weller HG, Gosman AD. A comparative study of subgrid scale models in homogeneous isotropic turbulence. Phys Fluids 1997;9:1416–29.